Reference
NBS
PUBLICATIONS

A11102 516803

NAT'L INST OF STANDARDS & TECH R.I.C.
A11102516803
Hebner, Robert E/Report of tests on Jose
QC100 .U56 NO.86-3405 1986 V19 C.1 NBS-P

Report of Tests on Joseph Newman's Device

Robert E. Hebner
Gerard N. Stenbakken
David L. Hillhouse

U.S. DEPARTMENT OF COMMERCE
National Bureau of Standards
National Engineering Laboratory
Center for Electronics and Electrical Engineering
Electrosystems Division
Gaithersburg, MD 20899

June 1986

QC
100
.U56
86-3405
1986

. DEPARTMENT OF COMMERCE
IONAL BUREAU OF STANDARDS

NBS
RESEARCH
INFORMATION
CENTER

NBSIR 86-3405

REPORT OF TESTS ON JOSEPH NEWMAN'S DEVICE

Robert E. Hebner
Gerard N. Stenbakken
David L. Hillhouse

U.S. DEPARTMENT OF COMMERCE
National Bureau of Standards
National Engineering Laboratory
Center for Electronics and Electrical Engineering
Electrosystems Division
Gaithersburg, MD 20899

June 1986

U.S. DEPARTMENT OF COMMERCE, Malcolm Baldrige, *Secretary*
NATIONAL BUREAU OF STANDARDS, Ernest Ambler, *Director*

FOREWORD

This report fulfills a request by the U.S. Patent and Trademark Office that the National Bureau of Standards conduct tests on Joseph Newman's device as part of a lawsuit involving Mr. Newman and PTO. The tests were conducted following an agreement between PTO and NBS and were carried out in accordance with several court orders.

Specifically, NBS was asked to prepare a report on its tests, including:

> "(a) a copy of the final test plan including pictures of the working models;
>
> (b) a description of the credentials and qualifications of the NBS experts;
>
> (c) a description of the test equipment used and when and how it was calibrated;
>
> (d) a detailed description of the working models;
>
> (e) a detailed description of the conduct of the tests; and
>
> (f) the test results including the percentage of the input energy that is converted to output energy by each of Mr. Newman's working models."

The test plan was submitted before we began our tests and is on file with the United States District Court for the District of Columbia. The remaining items are covered in this report.

Our results are clear and unequivocal. As the report states, "At all conditions tested, the input power exceeded the output power. That is, the device did not deliver more energy than it used."

NBS believes that this report is responsive to the several court orders. It is also clear that our test results are entirely consistent with well-established laws of physics. NBS can think of no way that this or any other device could be constructed or operated to violate either the principle of conservation of energy or the Second Law of Thermodynamics.

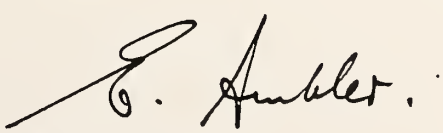

Ernest Ambler
Director

TABLE OF CONTENTS

STATEMENT OF FINDINGS i

1. Introduction 1

2. Experimental Approach 1
   2.1 Introduction 1
   2.2 Brief Description of Device under Test 4
   2.3 Input Power Measurements 6
   2.4 Output Power Measurements 11

3. Results 14

4. Consistency Checks 18
   4.1 Introduction 18
   4.2 Assessment of Frequency Dependence of Input Power 18
   4.3 Approximate Determination of Input Power 19
   4.4 Measurement of Input and Output Power Using the Sampling Wattmeter 19
   4.5 Spectrum Analysis 19
   4.6 Direction of Power Flow 19
   4.7 In Situ Measurement of the Output from a Signal Generator 19

5. Uncertainty Estimates 20
   5.1 Introduction 20
   5.2 Uncertainty and Offset in Input Power Measurements 21
   5.3 Uncertainty and Offset in Output Power Measurements 22
   5.4 Offset and Uncertainty in Efficiency Determination 23

6. Conclusions 24

7. References 24

Appendix 25

STATEMENT OF FINDINGS

This report describes electrical measurements performed by the National Bureau of Standards on Joseph Newman's device. The tests were conducted between March and June 1986 at the request of the U.S. Patent and Trademark Office in accordance with several court orders. As a Federal science and engineering research laboratory that specializes in measurements and is responsible for maintaining U.S. standards for electricity, NBS has extensive experience and facilities for measuring the performance of electrical equipment.

The purpose of the measurements was to test the inventor's claim that the output power from the device was greater than the power which was supplied to the device from a battery pack. NBS was not requested to examine the theory behind the operation of the device.

The tests consisted of electrical measurements of the power drawn from the battery pack by the device (input power) and separate as well as simultaneous measurements of the output power. These measurements were done with several different sets of conventional, well-documented test instruments. Due to the specialized nature of the equipment, however, the instrumentation would not generally be found in most research laboratories. The electrical characteristics of the device, especially the sharp spikes in input and output waveforms, necessitated a variety of extensive and careful measurements and experimental checks to ensure that valid data resulted. Equipment selection was critical.

The device's efficiency -- defined as the ratio of output power to input power -- varied depending on the voltage, load on the device, and the degree of degradation of the tape on the commutator of the device. If the device simply transferred the power from the batteries to the load, its efficiency would be 100 percent; in no case did the device's efficiency approach 100 percent.

<u>At all conditions tested, the input power exceeded the output power. That is, the device did not deliver more energy than it used.</u>

Report of Tests on Joseph Newman's Device

1. Introduction

This report describes results of tests performed between March 1986 and June 1986 on Joseph Newman's device. The purpose of the testing was to determine if the output power from the device was greater than the power which was put into the device from the battery pack. This report describes the experimental tests which were performed and summarizes the results.

This report describes a set of test results on a single device. NBS was not requested to examine the theory behind the operation of the device.

A photograph of the device which was tested is shown in figure 1. The system, as tested, consisted of a battery pack, a commutator which was mechanically connected to a rotating permanent magnet, and a coil of wire. The National Bureau of Standards provided the resistive load which was connected in parallel with the coil. Figure 1 does not show the battery pack and the load. The commutator reversed the polarity of the battery connection twice during each rotation of the magnet. In addition, twenty-four times during each rotation it connected the battery to and disconnected it from the coil of wire and the load. Consequently the output waveform was a series of pulses as is shown in figure 2.

The tests consisted of electrical measurements of the net power drawn from a battery pack by the device under test coupled with separate as well as simultaneous measurement of the power dissipated in a resistive load connected in parallel with the coil of the device.

Section 2 of this report describes the design of the tests and the selection of instrumentation used. Section 3 presents the measurement results. Sections 4 and 5 outline the consistency checks which were performed and provide estimates of the uncertainties associated with the various measurements performed. Section 6 presents conclusions and section 7 is a list of references cited in the report.

2. Experimental Approach

2.1 Introduction

Because this device was tested as a unique device, one element of the experimental approach was to assure the validity of the results by providing at least two independent, or nearly independent, measurements of both the input and the output power. To select the appropriate instrumentation, it was necessary to carry out preliminary investigations of the input and output waveforms. For both the input and the output, the waveform consisted of a series of twenty-four pulses, with the series repeating at approximately one- to two-second intervals. In addition, the crest factor (i.e. the ratio of the peak pulse amplitude to the root-mean-square value of the waveform) was found to be as large as about ten. Many types of instrumentation do not respond correctly over the observed frequency range and crest factor range, so the

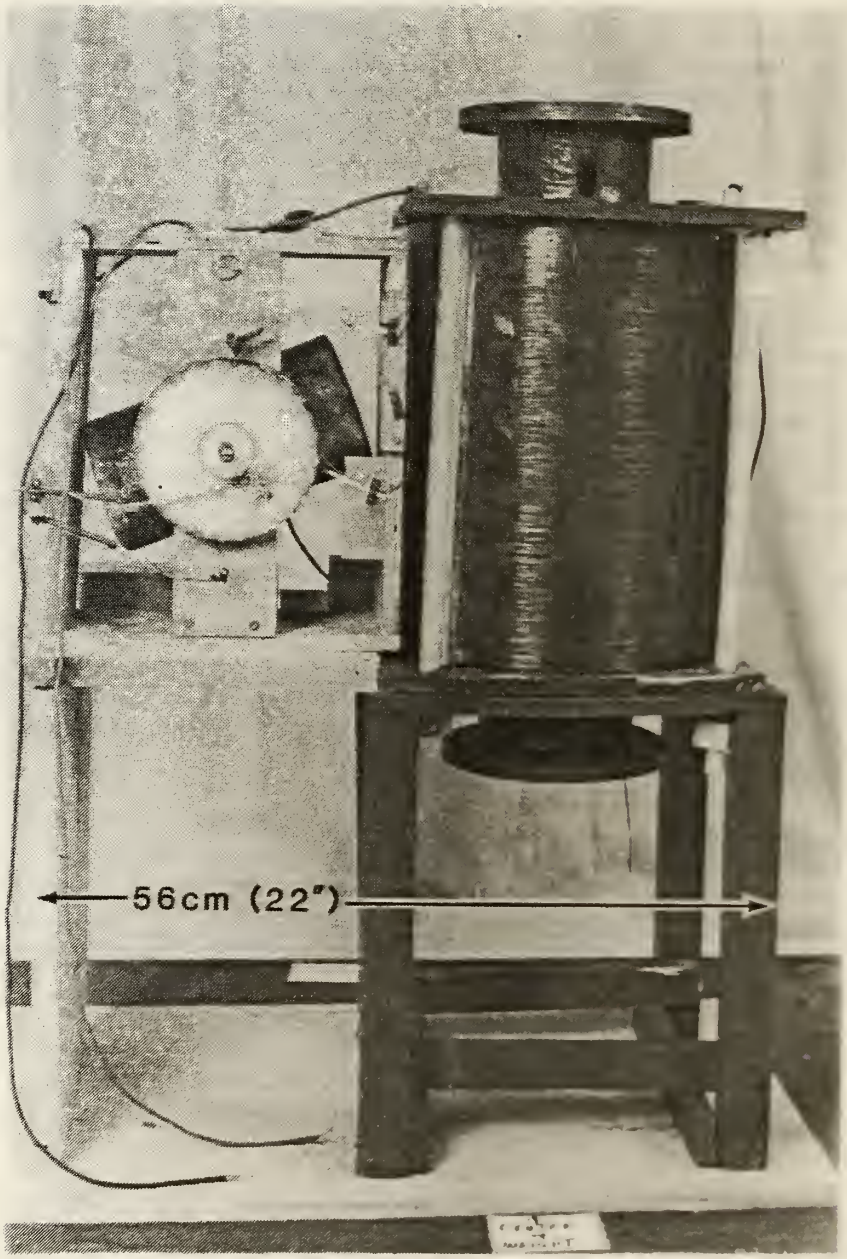

Figure 1. Photograph of Joseph Newman's device which was delivered to the National Bureau of Standards

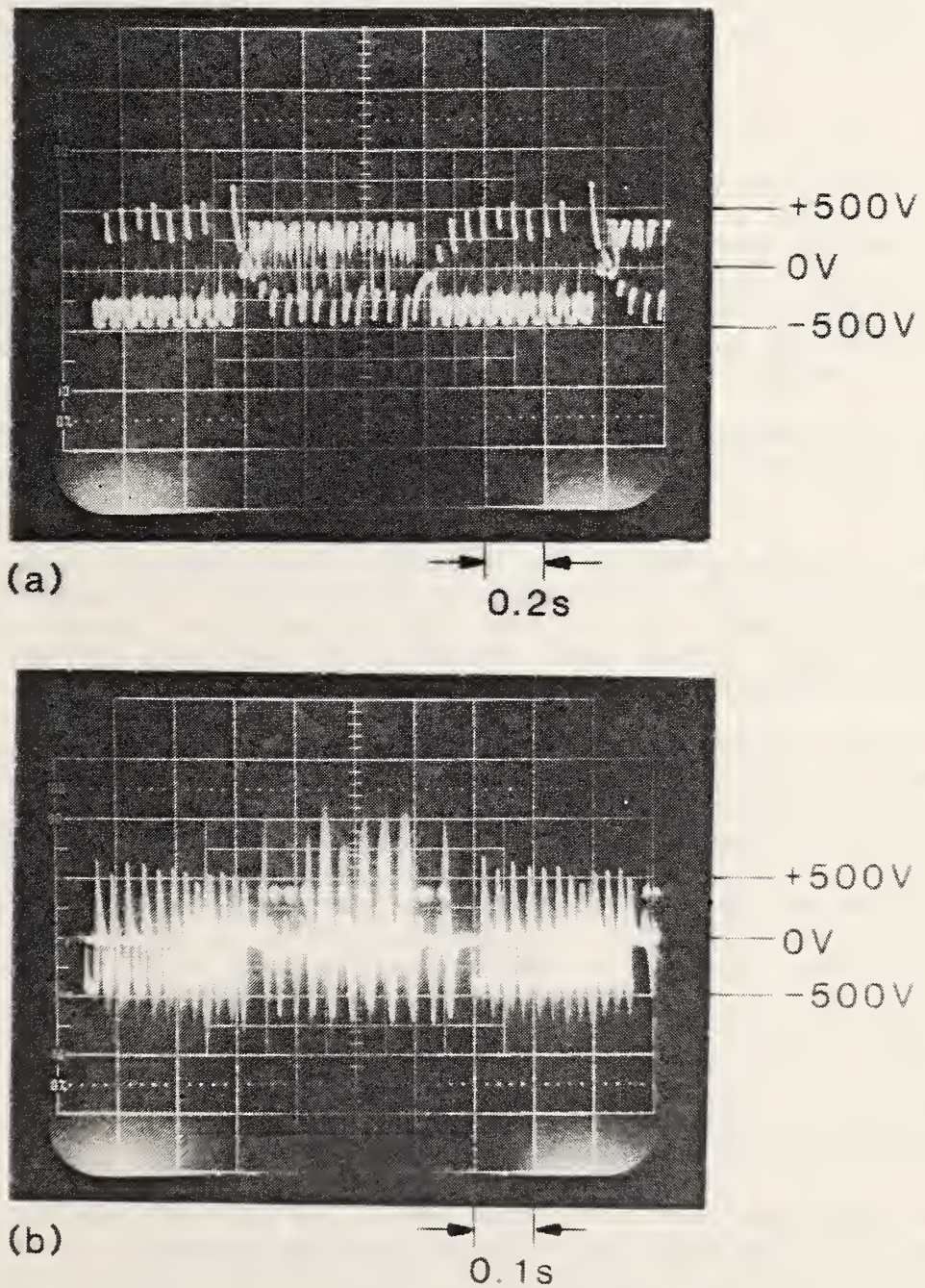

Figure 2. Photographs of two examples [(a) and (b)] of output waveform of device under test as measured using an oscilloscope

selection of the measurement equipment was especially important. The measurement approaches which were used at the National Bureau of Standards to acquire the data reported were appropriate for the waveforms measured.

A further consideration is that the waveforms changed with time, both in terms of the shapes of the individual pulses and in terms of the repetition interval. This variation results, at least in part, from the erosion of the tape (see section 2.2) on the commutator.

2.2 Brief Description of the Device under Test

The system which was evaluated consists of three primary components: the power source, a battery pack; the commutator, which is mechanically connected to a magnet which rotates during normal operation of the device; and the coil. The battery pack consists of 116 nine-volt batteries arranged in five sets of twenty batteries and one set of sixteen batteries. The batteries in each set are connected in series and external wiring is used to connect these various sets in series. The battery pack was provided by Mr. Newman.

During the testing, it was determined that one of the batteries in one of the sets was defective. After this battery was removed, the battery pack operated reliably.

Testing was performed at two different voltage levels. One of these levels was a nominal open circuit voltage of 1000 volts (the maximum available from the battery pack) and the other was a nominal open circuit voltage of 800 volts. These voltage levels decreased by about 50 to 150 volts when the battery pack was connected to the device.

A drawing of the commutator is shown in figure 3. The body of the commutator wheel is constructed from a plastic material. The outer edge of the wheel is covered by a metallic strip. This strip is split into two semicircles which are separated by small plastic spacers. Twelve pieces of tape are attached to one of the semicircles. These pieces of tape are arranged so that alternate, approximately equal, segments of the semicircle are covered and exposed. Two brushes contact the wheel about 180° apart. Each of these brushes is connected electrically to one of the two leads of the coil. There is a small slip ring on each side of the wheel. The sliding contact on one of the slip rings is connected to the grounded side of the battery. This slip ring is connected to the semicircle which does not have tape on it. The sliding contact on the other slip ring is connected to the positive terminal of the battery pack. This slip ring is connected to the semicircle which does have tape on it.

This commutator operates so that during one half of a revolution one side of the coil is connected to the anode (positive terminal) of the battery pack while the other side is connected to the grounded cathode (negative terminal) of the battery. During the other half of the revolution, the side of the coil which had been connected to the cathode is now connected to the anode and the side which had been connected to the anode is now connected to the grounded cathode. During each half cycle, the twelve pieces of tape alternately cause the battery anode to be connected to and disconnected from the coil.

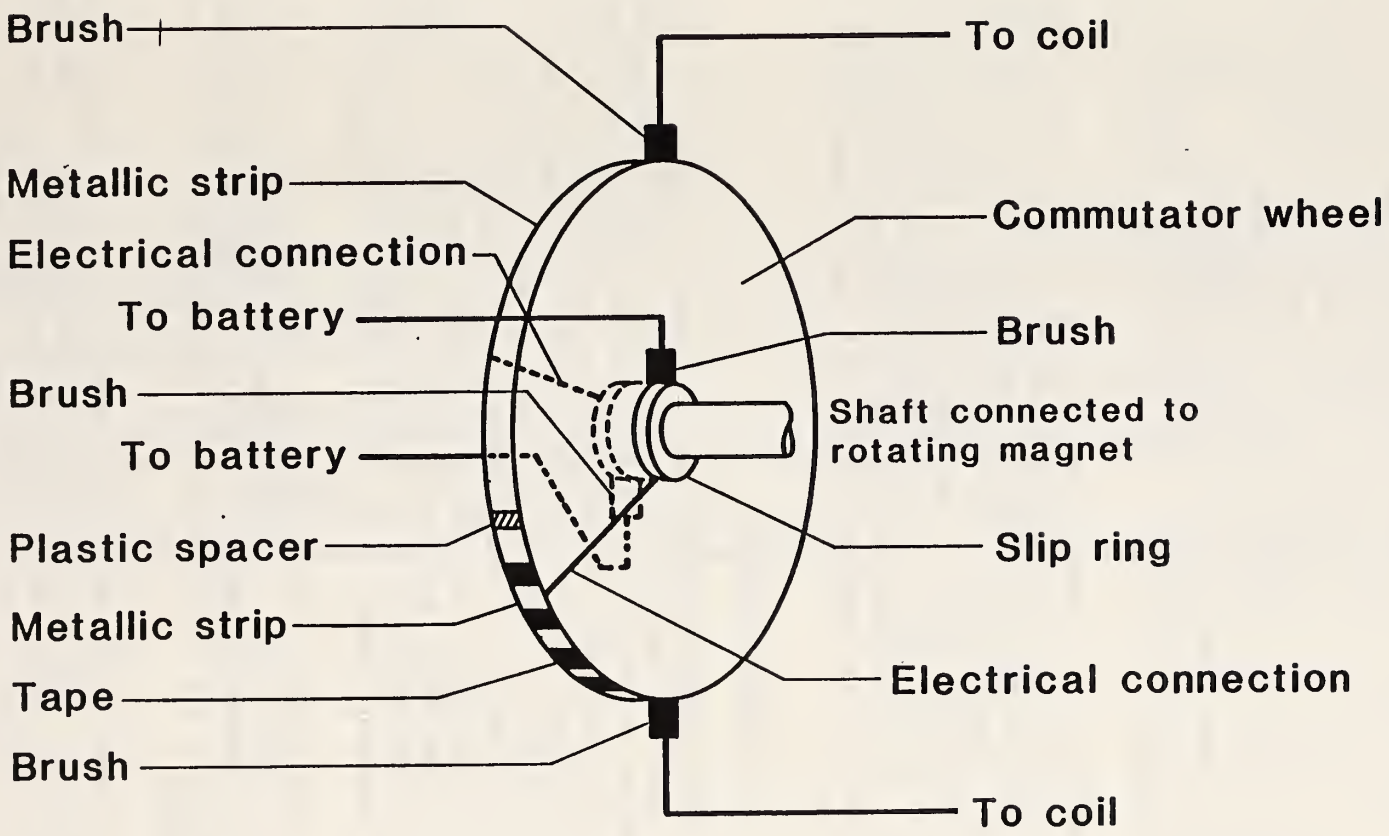

Figure 3. Schematic drawing of commutator

The commutator wheel is mechanically connected to a permanent magnet which is rotated by the magnetic field of the coil. The permanent magnet is supported along its axis of rotation by bolts which pass through holes in the wooden support structure. The device vibrated as its magnet rotated.

A small spark is produced each time either of the sliding contacts passes from a conducting surface to a tape-covered surface or a plastic spacer. After a period of operation, it was noted that this spark burns the insulating material. For this reason, one of the plastic spacers had to be replaced during the course of the testing and the tape had to be replaced frequently with fresh, cellulose acetate tape. It was noted that the efficiency of the device under test was dependent upon the condition of this tape (i.e. as the tape eroded, the efficiency of the device decreased). Two consequences of this behavior were that the device is not characterized by a single efficiency -- its efficiency is variable -- and that it was necessary to replace the tape frequently because the highest efficiency was obtained with fresh tape.

The coil appears to be constructed of many turns of fine wire. To characterize the coil, the impedance of the coil as a function of the frequency (when sinusoidal signals were applied) was measured. The resulting data are consistent with an interpretation that below about 100 hertz the coil acts as an inductor, with an inductance of about 2500 henries, while above about 1000 hertz it acts as a capacitor, with a capacitance of about 850 picofarads. The structure of the response between 100 hertz and 1000 hertz is presumably due to the combination of resistance, capacitance, and inductance within the coil.

2.3 Input Power Measurements

The input power measurement system, as shown in figure 4, consists of a voltage divider (R_1 and R_2), a current shunt (R_{CS}), and appropriate instrumentation to obtain the product of the voltage and current waveforms. The voltage divider has a high impedance network which consists of a 5-megohm resistor and a parallel capacitance of 6 picofarads. The low impedance arm of the divider is a 50-kilohm resistor. The load on the divider is approximately 6 meters of coaxial cable to a low-pass filter and to two measuring instruments, each having an input impedance of 1 megohm. The resistance of the high impedance element was selected to minimize the power dissipated in the divider. The parallel capacitance was then chosen to obtain a uniform frequency response, to within ±2%, for frequencies up to 5000 hertz.

A current shunt having a resistance of 100.1 ohms was selected to provide appropriate signal levels. Measurements showed that for both direct current and 50-hertz alternating current signals, the shunt maintained its nominal value to within a few tenths of a percent for currents in the range from 1 to 50 milliamperes.

The output signals from the divider and shunt were measured using both a sampling wattmeter and an analog-multiplier wattmeter. The sampling wattmeter was a wideband precision meter developed by the National Bureau of Standards [1]. A block diagram of the wattmeter is shown in figure 5. The instrument has two voltage input channels, and it can calculate and display the average of the product of the two input voltages. One of these input voltages, V_2, is derived from the current shunt and the other, V_1, is derived from the voltage

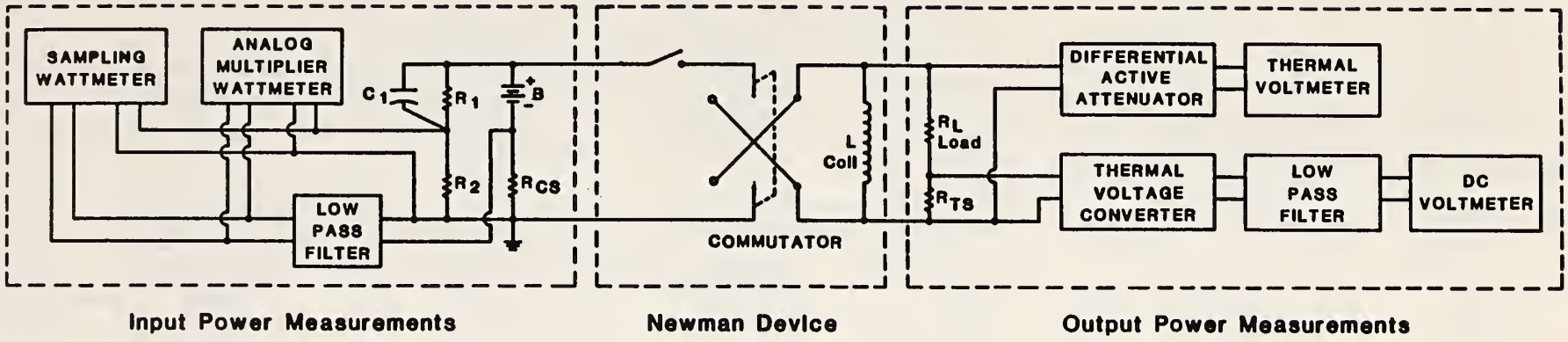

Figure 4. Schematic drawing of Newman device and input and output power measurement circuits

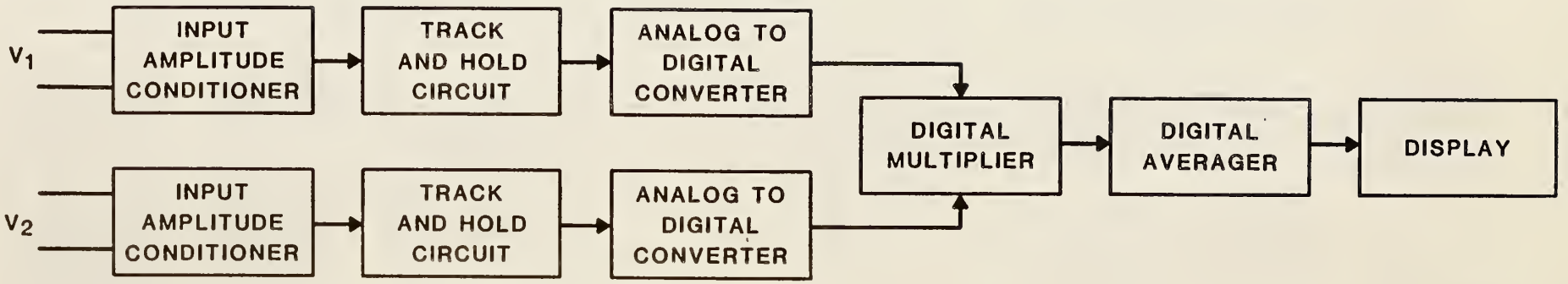

Figure 5. Block diagram of sampling wattmeter

divider. The displayed value, with proper scaling, shows the amount of power drawn from the battery. Using appropriate software, the sampling wattmeter can also be used to measure either the average or the root mean square (rms) value of a signal applied to either channel.

Each input channel consists of the three circuit elements shown schematically in figure 5. First, the input-amplitude-conditioner circuit scales the input signal to a level which is appropriate for the remaining circuitry. Second, the track-and-hold circuit samples an instantaneous value from the input circuit and holds that value at its output. Third, the analog-to-digital converter transforms the value of the analog signal to an appropriate digital signal. As soon as the digital signal is determined and transmitted to the following circuitry, the track-and-hold circuit takes a new sample of the input signal which is transformed into the next digital value. Thus, a sequence of digital signals flows from each channel and the value of a specific digital signal is proportional to an instantaneous sample of an input signal.

The digital signals from each channel are applied to the inputs of a digital multiplier. The multiplier calculates the product of the two signals. These product values are transmitted to a digital averager which determines the average value of a large number of these inputs. The average values, which are proportional to the power drawn from a source or delivered to a load, are displayed on the front panel.

The analog-multiplier wattmeter is a commercial instrument which was modified so that it could accommodate an external current shunt. Originally, the instrument had a voltage input channel and a current input channel. The input current was passed through an internal current shunt to generate a voltage signal of the proper amplitude. The signal on the input voltage channel was scaled using a voltage divider.

As shown in the schematic diagram of this instrument in figure 6, these two signals are applied to the input terminals of an analog multiplier circuit. The output of the multiplier is proportional to the product of the two input signals. This signal is filtered using a low-pass filter and applied to the input of an analog-to-digital converter. The digital output is simultaneously directed to both a front panel digital display and to a digital interface circuit. For most of the data taken during this investigation, the digital output was recorded using a computer to "read" the signal at the digital interface connector. This digital signal is proportional to the power drawn from a source or delivered to a load.

As figure 6 shows, the instrument was modified for this application by disconnecting the voltage signal from the internal current shunt to the multiplier circuit. In place of the signal from the internal shunt, the signal from a new voltage attenuator is applied to the multiplier circuit. This attenuator receives its input V_2 from the external current shunt R_{CS}. Thus, with proper scaling, the value of the display shows the power drawn from the battery.

Because of some very large spikes in the current waveform, a low-pass filter was used on the current signal to both the sampling wattmeter and the analog-multiplier wattmeter. The filter prevented the spikes from producing a

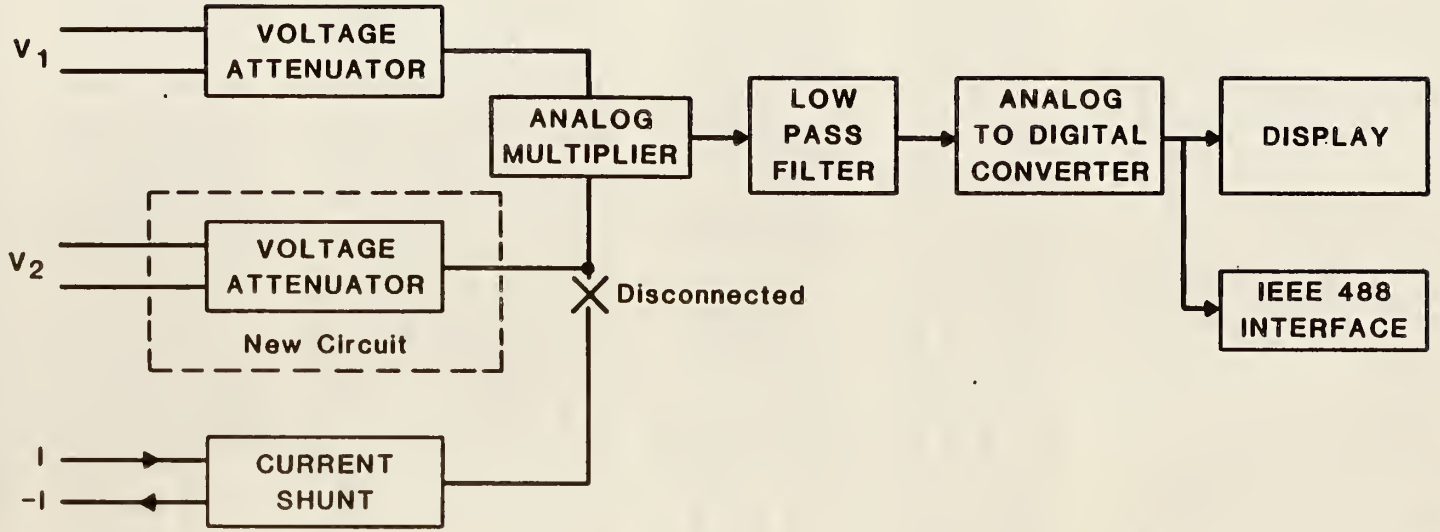

Figure 6. Block diagram of analog-multiplier wattmeter

significant measurement error. The use of the filter results in the determination of the input power which is lower than the true value. To determine the signal loss due to this circuit, matching sets of high-pass and low-pass filters were constructed. The results of measurements using these filters are given in section 4.2. Figure 7 is a schematic diagram of the high-pass and the low-pass filters. The filters were constructed using a resistance of 1000 ohms and a capacitance of 20 nanofarads.

2.4 Output Power Measurements

The output power was the power dissipated in a resistive load R_L connected in parallel with the coil of the device under test, as shown in figure 4. Two values of resistive load were constructed: nominally 50,000 ohms, and 200,000 ohms. By using series and parallel combinations of resistors of these values tests were run at nominal loads of 400,000 ohms, 200,000 ohms, 150,000 ohms, 100,000 ohms, and 50,000 ohms. Most of the data, however, were taken at 200,000 ohms or 50,000 ohms. The 200,000-ohm level was selected because at this point the power dissipated in the load and the power dissipated in the device under test were approximately equal. The 50,000-ohm level was selected as the smallest value of the resistance that could be used routinely without potentially damaging the device; one of the goals of the test program was to perform only nondestructive measurements. A significant source of potential damage was the vibration of the device, which increased as the value of the load resistance decreased.

To determine the power dissipated in the load resistor R_L, three different approaches were used. The first was the differential active attenuator diagrammed in figure 8. This attenuator, which was constructed at the National Bureau of Standards, produced a signal at its output which was proportional to the voltage difference across the resistive load. This output voltage was measured using a commercially available digital voltmeter. This voltmeter incorporated a thermal element. A thermal element [2] is among the basic tools used in the determination of the rms (root-mean-square) value of a voltage waveform. The thermal element consists of two primary components: a heater which changes temperature with changes in the current being passed through the element and a thermocouple to produce a voltage which is proportional to the temperature. The power dissipated in the load is the square of the rms voltage across the load resistor divided by the resistance value of the resistor.

The second approach uses a thermal element which is not a part of a commercial instrument. In this case, a shunt resistor R_{TS}, nominally 100 ohms for a 50,000-ohm load, is placed in parallel with the thermal element. This combination is then connected in series with the load. In this configuration, the thermal element is "floating", i.e. depending on the instantaneous position of the commutator, the thermal element may be near ground potential or it may be near the maximum voltage of the battery. The output from the thermocouple in the thermal element was passed through a low-pass filter and was measured using a digital voltmeter. This thermal element is calibrated by applying a known voltage signal across the thermal element and its associated resistor and recording the output voltage from the thermocouple. The voltage across the load resistor is calculated by recording the output from the thermocouple, computing the voltage across the thermal element and the associated resistor from the calibration data, and calculating the voltage

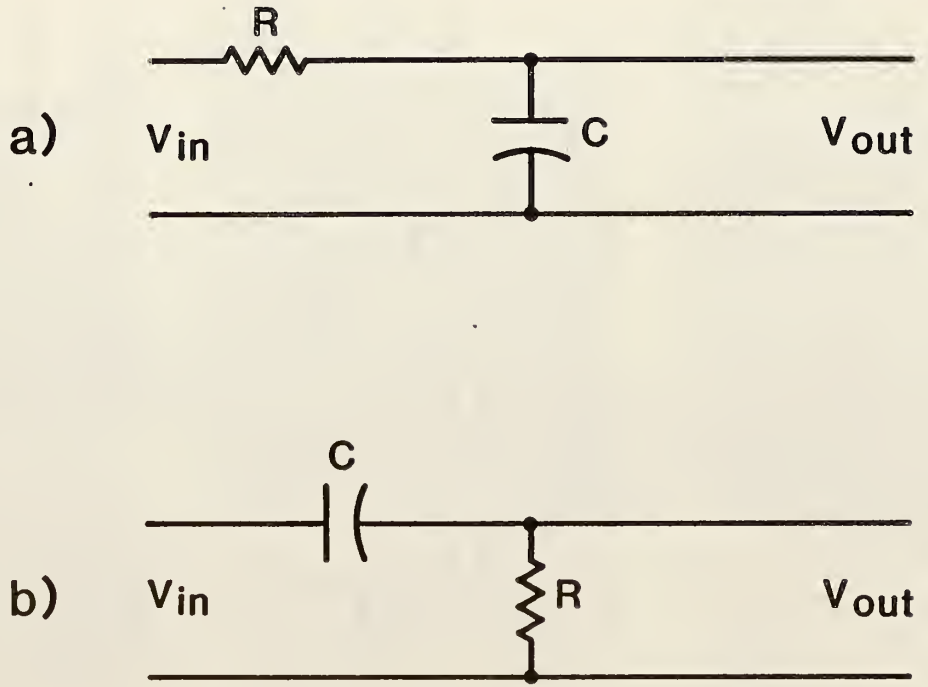

Figure 7. Low-pass (a) and high-pass (b) filters

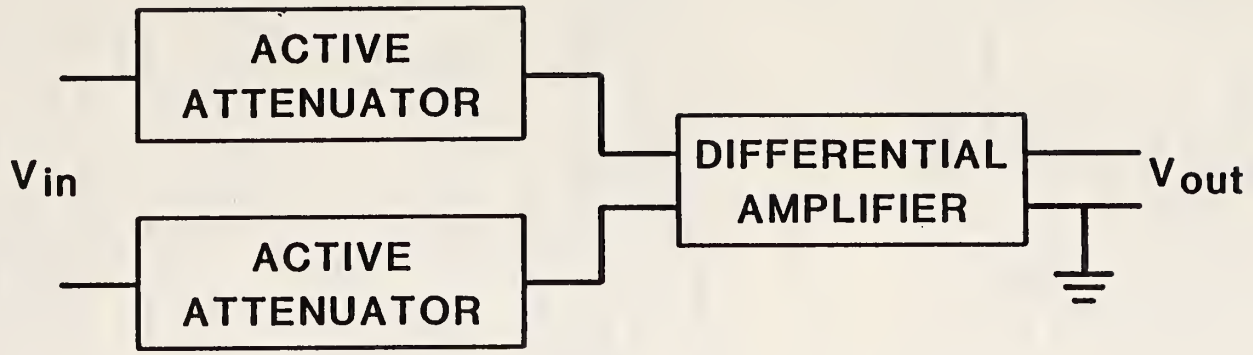

Figure 8. Block diagram of differential active attenuator

across the load resistor by multiplying the thermal element voltage by the resistance ratio of the load resistor to the parallel combination of the shunt resistor and the resistance of the thermal element. The power is then obtained by squaring this voltage and dividing it by the value of the load resistance.

The third measurement technique used is shown in figure 9. This resistance configuration had the advantage of being convenient to use and conceptually simple. Because one side of the coil was nearly always connected to ground, significant current would flow only through the 200,000-ohm resistor which was connected to the side of the coil which was not connected to ground. Thus, as the commutator reversed the connections to the coil, the two resistors would alternately carry current. But, as is discussed in section 5.3, because the switching sequence of the commutator disconnected the coil from ground once each rotation, this measurement technique always produced a value of the output power which was too large so that the measured value of the efficiency was always greater than the true value. This configuration was called the BI-200 because it was composed of two load resistors R_{L1} and R_{L2} each having a resistance of 200,000 ohms.

3. Results

The results of the various measurements of the input power and the output power are summarized in Table 1. The efficiency is defined as the ratio of the output power to the input power expressed in percent and the internal loss is defined as the difference between the input power and the output power. It should be noted that the efficiency and the internal losses are two related measures of the effectiveness of the device.

The two measured values of the input power were averaged to obtain the uncorrected efficiency data and the internal losses. In the remarks column in Table 1, "Atten." indicates that the output measurement was made using the active attenuator, "TE" indicates that the output measurement was made using the thermal element and shunt, and "BI-200" indicates that the output measurement was made using the BI-200 load, in parallel with other resistors as necessary. The quantities "800 V" and "1000 V" are the nominal open circuit voltages of the battery pack. The entries in the column labeled "uncorrected efficiency data" are the ratios of the measured powers while the "corrected efficiency results" have been corrected for the known offsets. This column shows the estimated uncertainty of the measurements.

The corrections and uncertainties associated with these measurements are discussed in section 5. For convenience, the results of that discussion are summarized here. For the active attenuator, it is estimated that the true efficiency is within ±4% of the measured value. The values measured using the thermal element are estimated to be 5±4% larger than the true value. Similarly, the values measured with the BI-200 load are about 10±6% larger than the true values. This means, for example, that if the value of the efficiency measured using the active attenuator is listed as 41% the true value is between 37% and 45%. If the value taken using the thermal element is listed as 54%, the true value is between 45% and 53%. Finally, if the value was measured as 77% using the BI-200 load, then the true value is between 61%

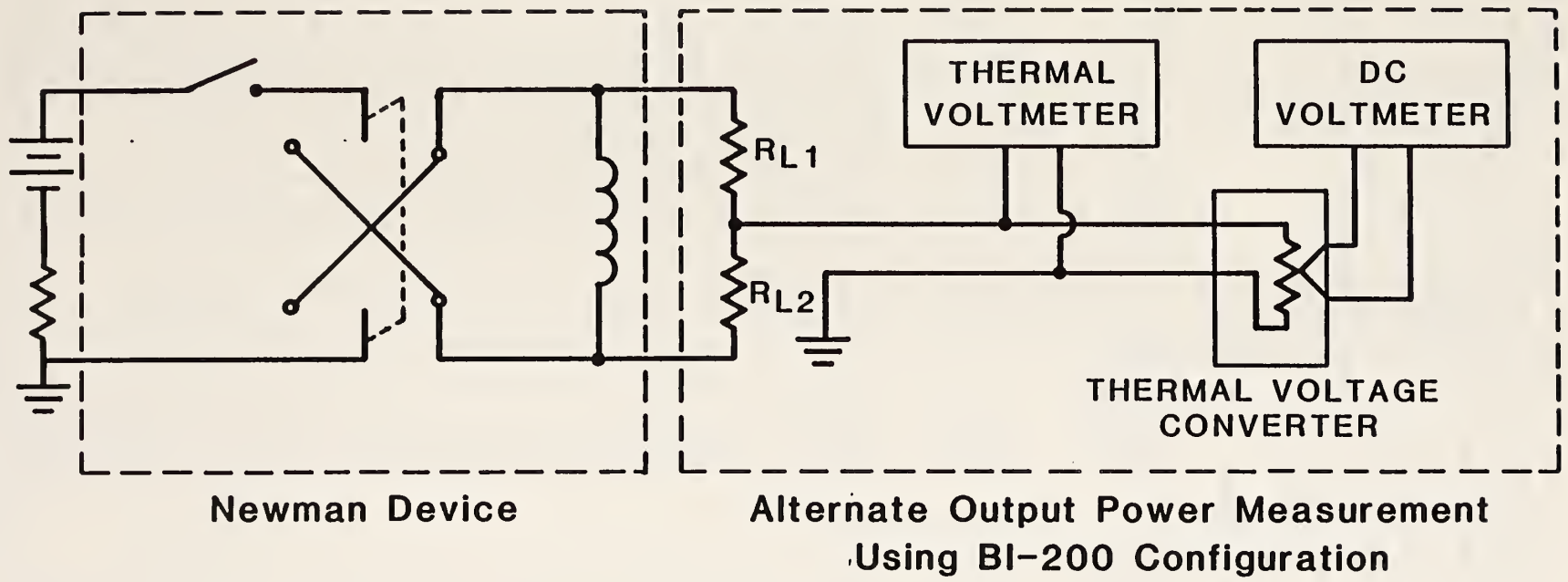

Figure 9. Schematic diagram of measurements using BI-200 Load

and 73%. No corrected efficiency is given for the two measurements made using the BI-200 as a load and the attenuator to measure the voltage across the load because no experimental data were taken to provide direct support for any corrections or uncertainty estimates. From other data and from a knowledge of the circuit, it is estimated that the uncertainty is no smaller than was obtained for the attenuator measurements using other loads and that the offset should be smaller than that obtained using the BI-200 alone. The variation of the efficiency under nominally identical conditions is greater than would be expected due to measurement uncertainty because, as was mentioned in section 2.2, the efficiency is not constant.

Table 1. Summary of measurement results

LOAD RESISTOR	UNCORRECTED EFFICIENCY DATA	CORRECTED EFFICIENCY RESULTS	INTERNAL LOSSES	REMARKS
Ohms	Percent	Percent	Watts	
400,000	29	29 ± 4	2.5	Atten., 800 V
	30	30 ± 4	2.5	Atten., 800 V
	34	29 ± 4	2.4	TE, 800 V
	35	30 ± 4	2.3	TE, 800 V
200,000	41	31 ± 6	3.0	BI-200, 800 V
	39	29 ± 6	3.9	BI-200, 800 V
	45	35 ± 6	2.4	BI-200, 800 V
	44	34 ± 6	2.4	BI-200, 800 V
	27	---	3.1	BI-200 + Atten., 800 V
	38	28 ± 6	2.7	BI-200, 800 V
	27	27 ± 4	3.0	Atten., 800 V
	39	29 ± 6	2.5	BI-200, 800V
	27	27 ± 4	3.0	Atten., 800 V
	45	35 ± 6	2.6	BI-200, 800 V
	39	39 ± 4	2.6	Atten., 800 V
	44	34 ± 6	2.5	BI-200, 800 V
	39	39 ± 4	2.7	Atten., 800 V
	45	40 ± 4	2.3	TE, 800 V
	42	42 ± 4	2.3	Atten., 800 V
	45	40 ± 4	2.2	TE, 800 V
	42	42 ± 4	2.3	Atten., 800 V
	35	30 ± 4	2.5	TE, 800 V
	33	33 ± 4	2.6	Atten., 800 V
	35	30 ± 4	2.5	TE, 800 V
	33	33 ± 4	2.6	Atten., 800 V
	41	31 ± 6	2.6	BI-200, 800 V
	36	36 ± 4	2.9	Atten., 800 V
	34	---	3.1	BI-200 + Atten., 800 V
	45	35 ± 6	2.4	BI-200, 800 V
	39	29 ± 6	3.9	BI-200, 1000 V
	46	41 ± 4	2.4	TE, 1000 V
	41	41 ± 4	2.7	Atten., 1000 V
	45	40 ± 4	2.5	TE, 1000 V
	40	40 ± 4	2.7	Atten., 1000 V

(continued)

Table 1. Summary of measurement results (continued)

LOAD RESISTOR Ohms	UNCORRECTED EFFICIENCY DATA Percent	CORRECTED EFFICIENCY RESULTS Percent	INTERNAL LOSSES Watts	REMARKS
150,000	44	34 ± 6	3.0	BI-200, 800 V
	48	38 ± 6	3.7	BI-200, 1000 V
	33	33 ± 4	3.4	Atten., 1000 V
	37	32 ± 4	3.2	TE, 1000 V
	32	32 ± 4	3.3	Atten., 1000 V
	37	32 ± 4	3.1	TE, 1000 V
100,000	54	49 ± 4	2.3	TE, 800 V
	46	46 ± 4	2.6	Atten., 800 V
	53	48 ± 4	2.3	TE, 800 V
	46	46 ± 4	2.6	Atten., 800 V
	52	47 ± 4	2.7	TE, 1000 V
	50	50 ± 4	3.0	Atten., 1000 V
	50	45 ± 4	3.1	TE, 1000 V
	47	47 ± 4	3.1	Atten., 1000 V
50,000	53	53 ± 4	3.1	Atten., 800 V
	55	50 ± 4	3.0	TE, 800 V
	52	52 ± 4	3.3	Atten., 800 V
	54	49 ± 4	3.4	TE, 800 V
	50	50 ± 4	3.2	Atten., 800 V
	54	49 ± 4	3.1	TE, 800 V
	51	51 ± 4	3.2	Atten., 800 V
	55	50 ± 4	3.0	TE, 800 V
	59	59 ± 4	2.6	Atten., 800 V
	63	58 ± 4	2.4	TE, 800 V
	59	59 ± 4	2.6	Atten., 800 V
	64	59 ± 4	2.3	TE, 800 V
	53	53 ± 4	3.0	Atten., 800 V
	59	54 ± 4	2.7	TE, 800 V
	53	53 ± 4	3.0	Atten., 800 V
	59	54 ± 4	2.8	TE, 800 V
	59	59 ± 4	2.6	Atten., 800 V
	64	59 ± 4	2.4	TE, 800 V
	60	60 ± 4	2.5	Atten., 800 V
	64	59 ± 4	2.4	TE, 800 V
	40	40 ± 4	4.9	Atten., 1000 V
	54	49 ± 4	3.7	TE, 1000 V
	41	41 ± 4	4.9	Atten., 1000 V
	55	50 ± 4	3.6	TE, 1000 V
	73	63 ± 6	2.9	BI-200, 800 V
	77	67 ± 6	2.4	BI-200, 1000 V

When the 50,000-ohm load resistor was used with the BI-200, the load on the device was a parallel combination of the two systems. Therefore, the value of

the load was 40,000 ohms during most of the cycle and 44,000 ohms when the commutator disconnected the ground from the coil without disconnecting the battery.

4. Consistency Checks

4.1 Introduction

In the development of measurement techniques, it is necessary to provide certain checks to verify that unanticipated errors have not corrupted the data. For conventional measurement systems, an experienced metrologist will identify any deviations from the normal behavior for a particular class of device. For one-of-a-kind devices, it is customary to make some explicit checks to provide additional assurance that the measurement results are correct within the stated uncertainties. The following paragraphs describe such consistency checks for measurements made on the Newman device.

4.2 Assessment of the Frequency Dependence of the Input Power

As mentioned previously, the input power was measured using a low-pass filter on the input current channel. To determine the effect of the filter, matched sets of filters were constructed. One set was a pair of high-pass filters; the other set was a pair of low-pass filters. Both sets had 3-dB points (50% reduction) at 8000 hertz. Thus if one were measuring the power using the low-pass filters, one would be measuring approximately the power at frequencies below 8000 hertz and when using the high-pass filters, the power above 8000 hertz. The results of such measurements are summarized in Table 2.

Table 2. Effect of high-pass and low-pass filters on input power measurements using the sampling wattmeter on various ranges for the current channel

FILTER	CURRENT RANGE Arbitrary Units	POWER Watts
High Pass	10	66×10^{-3}
	20	84×10^{-3}
	50	108×10^{-3}
	100	110×10^{-3}
Low Pass	20	3.7
	50	3.9

Two observations can be drawn from these data. First, the power measured using the high-pass filters is less than 3% of the power measured using the low-pass filters. This result shows that the measured efficiency should be less than 3% larger than the true efficiency of the device under test. Second, the measured power using the high-pass filters increased as the current range increased. This trend suggests that, in this frequency range, there are high amplitude signals which saturate the input circuit and produce measurement errors at the lower ranges. It is not feasible to measure power using the higher current ranges because most of the signal is at lower

amplitude and large measurement errors can occur if low amplitude signals are measured using a high amplitude range. Thus, to minimize and to control measurement error, the data were taken using a low-pass filter.

4.3 Approximate Determination of the Input Power

Because the battery voltage is nearly constant (implying that the average voltage is nearly equal to the rms voltage), the product of the average current and the voltage should nearly equal the input power. To test this relationship, measurements were made using the sampling wattmeter to determine the input power, the rms voltage, and the average current. The results, which show that the product of the voltage and the current approximates the measured power, are summarized in Table 3.

Table 3. Comparison of power measurement to the current-voltage product in the determination of the input power

VOLTAGE RANGE	CURRENT RANGE	V_{rms}	I_{ave}	MEASURED POWER	$V_{rms} x I_{ave}$
Arbitrary Units	Arbitrary Units	Volts	Amperes	Watts	Volt-Amperes
2	2	806	5.2×10^{-3}	3.9	4.2
2	5	805	5.3×10^{-3}	4.1	4.3
2	10	802	5.3×10^{-3}	4.3	4.3
2	20	801	5.6×10^{-3}	4.4	4.5

4.4 Measurement of the Input and the Output Power Using the Sampling Wattmeter

In addition to the various tests, calibrations, and consistency checks performed, it is good practice to demonstrate that no systematic offsets occurred between the instrumentation used to measure the input power and that used to measure the output power. Measurements, therefore, were made to identify any significant offset. These consisted of input measurements using the sampling wattmeter and the analog-multiplier wattmeter followed by measurements of the output using the active attenuator. The signal from the attenuator was measured using the digital voltmeter (DVM) which was used in subsequent measurements and also by the sampling wattmeter. These measurements, summarized in Table 4, demonstrate that the various instruments gave about the same indication under the same conditions.

Table 4 Measurement of the input and the output using the sampling wattmeter

NOMINAL LOAD	MEASURED POWER (Watts)			
	Input		Output	
(Ohms)	Analog Multiplier	Sampling Wattmeter	DVM	Sampling Wattmeter
∞	3.5	3.5-4.2	--	--
500,000	--	--	0.7	0.7
50,000	8.2	7.7	4.2	4.2

4.5 Spectrum Analysis

A commercially available spectrum analyzer was used to measure the frequency content of the output voltage. This measurement was made using an NBS-developed divider which had a submicrosecond response time. The divider was attached to one terminal of the coil and the spectrum of the divider output voltage was measured. This measurement showed that most of the energy in the signal was in the frequency region below 50 hertz. At 500 hertz, the signal level was 1% of the low-frequency level.

These results were not used directly in the analysis of the data, but taken in conjunction with the other measurement results help to corroborate the observation that the power flow in the device is primarily a low frequency phenomenon.

4.6 Direction of Power Flow

The sign of the measured input power indicated that the battery pack was supplying net power to the device or, equivalently, that the device was not charging the battery pack. That is to say, power was flowing from the battery to the device-under-test and not from the device-under-test to the battery. To demonstrate that the signs were correct, a nominal 1-megohm resistor was placed in parallel with the device-under-test and the appropriate commutator brush was lifted so that no power was able to flow into the device. In this configuration the power was clearly flowing from the battery to the resistor and the measured polarity of the power flow was the same as it was when the battery powered the device-under-test.

4.7 In Situ Measurement of the Output from a Signal Generator

To assure that there were no unanticipated errors due to the arrangement and interconnection of the various measurement systems in the laboratory, an in situ calibration check was performed. All of the measurement systems were connected with cable runs in the same position used for measurement, except that no connections were made to the device-under-test. A signal generator was used to apply a signal to a parallel combination of the voltage divider with the current shunt, a shunt used with the thermal element and a 200,000-ohm load resistor, all connected in series. The power delivered to this combination was measured using the sampling wattmeter, the analog wattmeter, the thermal element, and the voltmeter used to measure the output from the active attenuator. Measurements using these systems differed by less than 1%.

5. Uncertainty Estimates

5.1 Introduction

In this section, the primary sources of measurement uncertainty are identified and their magnitudes are estimated. Two different kinds of uncertainty limits are discussed. One is an offset and the other is variations in the repeatability of the measurements which are represented as random errors. The sign convention used is that a positive offset produces a measured result which is larger than the true value of the parameter while a negative offset produces a measured result which is smaller than the true value. The

basis for the estimation of the offsets is described below. The limits for random variation, designated "±", are bounds which will include almost all repeated measurements. The following five measurements are evaluated: the input power using the sampling wattmeter; the input power using the analog-multiplier wattmeter; the output power using the active attenuator; the output power using the thermal element; and the output power using the BI-200 load.

5.2 Uncertainty and Offset in Input Power Measurements

The input power was measured using the sampling wattmeter and the analog-multiplier wattmeter. The primary sources of measurement error and their estimated magnitudes are listed in Table 5.

The low-pass filter introduces error because the higher frequency components of the power are measured with a consistent offset. As discussed in section 4.2, this error is such that the input power is consistently underestimated. The data support an estimate of -3% for this error.

The power dissipated in the voltage divider is between 0.1 and 0.2 watt depending upon the voltage level used. The percentage of the input power represented by this quantity depends on the load and the condition of the tape on the commutator. For this reason, this error was identified as being partially a systematic offset and partially a random error.

Table 5. Estimated offsets and uncertainties in input power measurement

ERROR SOURCE	SAMPLING WATTMETER	ANALOG-MULTIPLIER WATTMETER
Low-pass filter	-3%	-3%
Power dissipated in the voltage divider	+3%±2%	+3%±2%
Scale factor calibration	±0.4%	±0.2%
Frequency response of the voltage divider	±0.2%	±0.2%
Voltage dependence of the voltage divider	±0.2%	±0.2%
Averaging duration errors	±1.0%	±1.0%
Frequency response of the current shunt	±0.2%	±0.2%
Amplitude dependence of the current shunt	±0.2%	±0.2%
Induced signals	±1.0%	±1.0%

The calibration of the scale factors for both the sampling wattmeter and the analog wattmeter was performed by applying known signals from a commercially

available calibrator to the input terminals of the instruments. The values listed are the residual errors which were not accounted for in the calibration of the devices. It can be seen from Table 5 that the error due to this source was small compared to errors arising from other sources. This observation underscores the fact that a knowledge of the scale factors is necessary, but not sufficient, for a reliable measurement.

As noted in section 2.3, the calibration of the voltage divider indicated that variations in its frequency response are less than ±2% up to 5000 hertz. Because the bandwidth over which significant power is drawn is smaller than 500 hertz, a smaller error is estimated.

As a portion of the voltage divider calibration, the voltage dependence of its response was measured. These measurements indicated that the divider ratio changed by less than 0.1% as the voltage was increased from 300 volts to 1000 volts and was maintained at 1000 volts for five minutes.

To determine the average power, one must average over exactly one or an integral number of cycles or must average over a very large number of cycles so that the effect of any fractional cycle is negligible. The averaging duration error was estimated by noting the variation of successive measurements taken within a few minutes of each other. Since the averaging intervals are uncorrelated with the operation of the device, a major contributor to the difference in successive readings can be attributed to the averaging error. The measurement results obtained support an estimate of ±1% for this uncertainty.

The current shunt was a 100-ohm, non-inductive resistor. The stray capacitance is below the value which would affect the measured value of the input power by more than 0.2%.

As a portion of the calibration of the system, the amplitude dependence of the response of the current shunt was measured. The data obtained indicated that, over the range from 1 to 50 milliamperes, the response did not change by as much as 0.2%.

By use of appropriate grounding and shielding techniques, the induced signals, or "noise", did not contribute more than 1% of the measured input power. As will be seen in section 5.3, "noise" was a more significant factor in the output measurement.

5.3 Uncertainty and Offsets in Output Power Measurement

The output power was measured using an active attenuator, a thermal element, and a special resistive load called the BI-200. The estimated uncertainties for each of these measurement approaches are listed in Table 6.

The power dependence of the various loads was measured using a commercially available calibration source. No resistance value changed by as much as 0.6% from very low power to the maximum power measured in these tests.

The active attenuator was connected by short, shielded leads to the load. These shielded leads combined with a shielded attenuator and operation at relatively high voltage made this device less sensitive to induced signals

than other approaches. It is possible that the induced signal contribution is even smaller than estimated, but the short-term instability of the device under test makes it difficult to demonstrate that a smaller effect has been achieved. During some of the tests using the thermal element, the input to the thermal element was shorted and the device still indicated a power which was 3% to 8% of that which was measured without the short, indicating that this effect always gives rise to a measured value which is larger than the true value. That measurement is the basis for the induced signal offset and associated uncertainty estimates. The induced signal component using the BI-200 load results from the fact that during one polarity reversal of the commutator (and not both) the ground is disconnected from the coil before the battery is disconnected. In this situation, the coil has 400,000 ohms rather than 200,000 ohms in parallel with it. This contribution, will always yield a measured value of the output power which is larger than the true value. From photographs of the waveform and from comparison measurements, it is estimated that the offset is about 10% with an uncertainty of ±5%.

Table 6. Estimated offsets and uncertainties in the output power measurements

ERROR SOURCE	ACTIVE ATTENUATOR	THERMAL ELEMENT	BI-200
Power dependence of the load	±0.6%	±0.6%	±0.6%
Induced signals	±2%	+5±3%	+10±5%
Averaging duration errors	±1%	±1%	±1%
Scale factor errors	±0.6%	±0.6%	±0.2%
Frequency response of loads	±0.3%	±0.3%	±0.3%

The considerations which contributed to the assignment of averaging duration errors and scale factor errors are the same as those for input error measurement. In addition, an in situ check of the thermal element and the active attenuator was performed by applying a known voltage to the resistive load with the device-under-test disconnected. Each measurement system agreed with the input value to within 1%.

The contribution of the frequency response of the loads was estimated from comparisons of the direct current and 50-hertz calibration of the systems. These data showed that the frequency dependence was less than 0.3%.

5.4. Offset and Uncertainty in Efficiency Determination

Adding the systematic offsets and calculating the square root of the sum of the squares of the random errors provides an estimate of ±2.5% for the uncertainty of the measurement of the input power for each instrument. Using the same approach to calculate the output offset and uncertainty yields an estimate of ±2.5% for the active attenuator, +5%±3% for the thermal element, and +10%±5% for the BI-200. To estimate the uncertainty in the efficiency determination, the square root of the sum of the squares of the random

components of the input and output uncertainties is computed and added to any net offset. In this way, the following offsets and uncertainties in the efficiency determination are obtained: active attenuator, ±4%; thermal element, +5%±4%; BI-200, +10%±6%. It should be emphasized that the uncorrected values of the efficiency in Table 1 obtained using the thermal element and the BI-200 are larger than the true values of the efficiency.

6. Conclusions

The device's efficiency -- defined as the ratio of output power to input power -- varied depending on the voltage, load on the device, and the degree of degradation of the tape on the commutator of the device. If the device simply transferred the power from the batteries to the load, its efficiency would be 100 percent; in no case did the device's efficiency approach 100 percent.

At all conditions tested, the input power exceeded the output power. That is, the device did not deliver more energy than it used.

7. References

[1] G. N. Stenbakken, "A Wideband Sampling Wattmeter," IEEE Trans. Power Appar. Sys., vol. PAS-103, pp. 2919-2926, 1984.

[2] E. S. Williams, "Thermal Current Converters for Accurate AC Current Measurement," IEEE Trans. Instrum. Meas., vol. IM-25, pp. 519-523, 1976.

APPENDIX

This appendix contains a description of the credentials and the qualifications of the authors of this report.

ROBERT E. HEBNER

EDUCATION:

St. Marys University, San Antonio, TX	B.S.--Physics, 1967
University of Missouri	M.S.--Physics, 1969
University of Missouri	Ph.D.--Physics, 1971

EMPLOYMENT HISTORY:

1978 - present	Supervisory Physicist, National Bureau of Standards
1973 - 1978	Physicist, National Bureau of Standards
1972 - 1973	Presidential Intern, National Bureau of Standards
1971 - 1972	Postdoctoral Position, University of Missouri

PROFESSIONAL ACTIVITIES:

Member, IEEE Subcommittee on High Voltage Test Techniques, 1974 - present.

Member, IEEE Task Force on Varistors and Avalanche Diode Protective Devices, 1977-78; Task Force Secretary, 1978

Technical Advisor, EPRI-sponsored Project to Measure Transients in Electrical Transmission Systems, 1977-1982

Consultant, Geophysical Fluid Dynamics Laboratory, Princeton University, concerning protection against power line surges, 1977

Chairman, IEEE Working Group on Liquid Insulation, 1979-81; Member, 1981-82

Member, NSF Review Panel for Engineering Research Equipment Grants, 1979

Member, ADCOM IEEE Electrical Insulation Society, 1982 - present

Member, Education Committee, IEEE Electrical Insulation Society, 1982 - present

Member of the Advisory Committee and Group Leader, NATO Advanced Study Institute; Fast Electrical and Optical Diagnostic Principles and Techniques, 1983

Member, National Research Council's Committee to Conduct an Assessment on Establishing Underwater Arcs and Flames, 1985

PROFESSIONAL SOCIETY MEMBERSHIPS:

American Association for the Advancement of Science
American Physical Society
Institute of Electrical and Electronics Engineers
Sigma Xi

Robert E. Hebner (continued)

PUBLICATIONS

1. R. E. Hebner and K. J. Nygaard, "Selective Depopulation of the $6^2S_{1/2}(F=3)$ - Level in Cesium," J. Opt. Soc. Am., vol. 61, p. 1455 (1971).

2. R. E. Hebner and K. J. Nygaard, "A New Method for Studying Model Behavior and Temperature Tuning of Pulsed Room-Temperature GaAs Lasers," Physica, vol. 58, p. 225 (1972).

3. Y. B. Hahn, R. E. Hebner, D. R. Kastelein, and K. J. Nygaard, "Channeltron Gain in Magnetic Fields," Rev. Sci. Instru., vol. 43, p. 1839 (1972).

4. R. E. Hebner and E. C. Cassidy, "Measurement of 60 Hz Voltages Using the Kerr Effect," Rev. Sci. Instru., vol. 43, p. 1839 (1972).

5. R. E. Hebner, J. D. Jones, and K. J. Nygaard, "GaAs Laser Experiments for the Undergraduate Laboratory," Am. J. Phys., vol. 41, p. 217 (1973).

6. E. C. Cassidy, R. E. Hebner, M. Zahn, and R. J. Sojka, "Kerr Effect Studies of an Insulating Liquid under Varied High Voltage Conditions," IEEE Trans. Elec. Insul., vol. EI-9, p. 43 (1974)

7. K. J. Nygaard, R. E. Hebner, J. D. Jones, and R. J. Corbin, "Photoionization of the $6^2P_{3/2}, _{1/2}$ Fine-Structure Levels in Cesium," Phys. Rev. A, vol. 12, p. 1440 (1975).

8. R. E. Hebner, E. C. Cassidy, and J E. Jones, "Improved Techniques for the Measurement of High Voltage Impulses using the Electro-optic Kerr Effect," IEEE Trans. Instru. Meas., vol. IM-24, p. 361 (1975).

9. M. Misakian and R. E. Hebner, "Kerr Coefficients of Polychlorinated Biphenyls and Chlorinated Naphalene," J. Appl. Phys., vol. 47, p. 4052 (1976).

10. R. E. Hebner, R. A. Malewski, and E. C. Cassidy, "Optical Methods of Electrical Measurement at High Voltage Levels," Proc. IEEE, vol. 65, p. 1524 (1977).

11. R. E. Hebner and M. Misakian, "Temperature Dependence of the Optical Kerr Coefficient of Nitrobenzene," J. Appl. Phys., vol. 50, p. 6016 (1979).

12. E. F. Kelley and R. E. Hebner, "The Electric Field Distribution Associated with Prebreakdown Phenomena in Nitrobenzene," J. Appl. Phys., vol. 52, p. 191 (1981).

13. E. F. Kelley and R. E. Hebner, "Prebreakdown between Sphere-Sphere Electrodes in Transformer Oil," Appl. Phys. Letters, vol. 38, p. 231 (1981).

Robert E. Hebner (continued)

14. E. F. Kelley and R. E. Hebner, "Electrical Breakdown in Composite Insulating Systems: Liquid-Solid Interface Parallel to the Field," IEEE Trans. Elec. Insul., vol. EI-16, p. 297 (1981).

15. R. E. Hebner, E. F. Kelley, E. O. Forster, and G. J. FitzPatrick, "Observation of Prebreakdown and Breakdown Phenomena in Liquid Hydrocarbons," J. Electrostatics, vol. 12, p. 265 (1982).

16. M. Zahn, E. O. Forster, E. F. Kelley, and R. E.Hebner,"Hydrodynamic Shock Wave Propagation after Electrical Breakdown," Journal of Electrostatics, vol. 12 p. 535-536, (1982).

17. E. F. Kelley and R. E. Hebner, "Electro-optic Measurement of The Electric Field Distribution in Transformer Oil, "IEEE Trans. Power App. and Systems, vol. PAS-102, p. 2092 (1983).

18. E. F. Kelley and R. E. Hebner, "Measurement of the Electric Field in the Vicinity of an Oil-Pressboard Interface Parallel to the Field, IEEE Trans. Elec. Insul., vol. EI-19, p. 519 (1984).

19. R. E. Hebner, E. Kelley, E. Forster, and G. FitzPatrick,"Observation of Prebreakdown and Breakdown Phenomena in Liquid Hydrocarbons II. Non-uniform Field Conditions," IEEE Trans. Elec. Insul., vol. EI-20, p. 281 (1985).

Interagency Reports

20. K. J. Nygaard and R. E. Hebner, "Cross Section for Photoionization of Excited Cesium Atoms," Office of Naval Research Contract N0014-69-C-0271, Technical Report 1, 1970.

21. K. J. Nygaard and R. E. Hebner, "Cross Section for Photoionization of Excited Cesium Atoms," Office of Naval Research Contract N00014-69-C-0271, Technical Report 2, 1971.

22. K. J. Nygaard and R. E. Hebner, "Cross Section for Photoionization of Excited Cesium Atoms," Office of Naval Research Contract N00014-69-C-0271, Technical Report 3, 1972.

23. E. C. Cassidy, R. E. Hebner, W. E. Anderson, and R. J. Sojka, "Development and Analysis of Techniques for Calibration of Kerr Cell Pulse-Voltage Measuring Systems VI," Sandia Corporation Order AL-72-67, NBSIR 10 945, 1972.

24. E. C. Cassidy, R. E. Hebner, R. J. Sojka, and M. Zahn, "Development and Analysis of Techniques for Calibration of Kerr Cell Pulse-Voltage Measuring Systems VIII," Sandia Corporation Order FAO-28-0734, NBSIR 73-403, 1973.

25. R. E. Hebner, R. J. Sojka, and E. C. Cassidy, "Kerr Coefficients Nitrobenzene And Water," USAF Project No. AFWL 74-067.

Robert E. Hebner (continued)

26. R. E. Hebner, E. C. Cassidy, and R. J. Sojka, "Development And Analysis of Techniques for Calibration of Kerr Cell Pulse-Voltage Measuring Systems VIII," Sandia Order No. FAO-28-0990, NBSIR 74-564, 1974.

27. R. E. Hebner, "Calibration of Kerr Systems Used to Measure High Voltage Pulses, " Sandia Order No. 51-931, NBSIR 75-774, 1975.

28. R. E. Hebner, "Electrical Measurement of High Voltage Pulses in Diagnostic X-Ray Units," Food and Drug Administration Order FDA-IAG 224-74-6039, NBSIR 75-775, 1975.

29. R. E. Hebner and M. Misakian, "Calibration of High Voltage Pulse Measurement Systems Based on The Kerr Effect," Sandia Order No. 02-8994, NBSIR 77-1317, 1977.

30. R. E. Hebner, D. L. Hillhouse, and R. A. Bullock, "Evaluation of A Multimegavolt Impulse Measurement System," Bonneville Power Administration Order No. 14-03-7029-M, NBSIR 79-1933, 1979.

31. R. H. McKnight and R. E. Hebner, "X-Cal -- A Calibration System for Electrical Measurement Devices Used with Diagnostic X-Ray Units," Department of Defense CCG Project 78-130, NBSIR 80-2072, 1980.

32. E. F. Kelley and R. E. Hebner, "Breakdown between Bare Electrodes with An Oil-Paper Interface," Department of Energy Grant No. EA-77-01-6010, NBSIR 80-2071, 1980.

33. R. E. Hebner, E. F. Kelley. J. E. Thompson, T. S. Sudarshan, and T. B. Jones, "1980 Annual 'Report: "Optical Measurements for Interfacial Conduction and Breakdown, Nat. Bur. Stand. (U.S.), NBSIR 81-2275 (1981).

Published Conference Papers

34. K. J. Nygaard and R. E. Hebner, "Photo-Excitation And Ionization Rates in Cesium," IEEE Thermionic Energy Conversion Specialist Meeting, October 26-29, 1970, pp. 325-326.

35. K. J. Nygaard and R. E. Hebner, "Two-Step Photoionization in Cesium Vapors," Thermionic Conversion Specialist Conference, San Diego, California, October 4-6, 1971, IEEE Conference Record, pp. 288-291.

36. E. C. Cassidy and R. E. Hebner, "Experimental Study of The Behavior of Nitrobenzene under Varied High Voltage Conditions," 1972 Annual Report Conference on Electrical Insulation and Dielectric Phenomena, Washington, DC, pp. 37-44, National Academy of Sciences.

Robert E. Hebner (continued)

37. R. E. Hebner, E. C. Cassidy, M. Zahn, and R. Sojka, "Electric Field Distributions And Space Charge Behavior in Nitrobenzene under Low Frequency Alternating Voltage," 1973 Annual Report Conference on Electrical Insulation and Dielectric Phenomena, Washington, DC, pp. 112-119, National Academy of Sciences.

38. R. E. Hebner and S. R. Booker, "A Portable Kerr System for The Measurement of High Voltage Pulses," Proceedings of 1975 IEEE SOUTHEAST CON, 2, pp. 3A-1-1 through 3A-5.1.

39. E. F. Kelley and R. E. Hebner, "Measurement of Prebreakdown Electric Fields in Liquid Insulants," 1978 Annual Report Conference on Electrical Insulation and Dielectric Phenomena, Washington, DC, pp. 206-212, National Academy of Sciences.

40. E. F. Kelley and R. E. Hebner, "Time Evolution of The Electric Field Associated with Prebreakdown Phenomena in Liquids," 1979 Annual Report Conference on Electrical Insulation and Dielectric Phenomena, Washington, D.C., pp. 203-211, National Academy of Sciences.

41. R. E. Hebner and S. Annestrand, "Evaluation of Calibration Techniques for Multimegavolt Impulses Dividers," Third International Symposium on High Voltage Engineering, Milan, Italy, 42.18 pp. 1-4, 1979.

42. R. E. Hebner, E. F. Kelley, E. O. Forster, and G. J. FitzPatrick, "Observations of Prebreakdown and Breakdown Phenomena in Liquid Hydrocarbons II. Point-Plane Geometry," 1981 Annual Report Conference on Electrical Insulation and Dielectric Phenomena, pp. 377-389, (1981).

43. R. E. Hebner, E. F. Kelley, E. O. Forster, and G. J. FitzPatrick, "Observations of Prebreakdown and Breakdown Phenomena in Liquid Hydrocarbons," 7th International Conf. on Conduction and Breakdown in Dielectric Liquids, Berlin, West Germany, pp. 177-181 (1981).

44. M. Zahn, E. O. Forster, E. F. Kelley, and R. E. Hebner, Hydrodynamic Shock Wave Propagation after Electrical Breakdown," 7th International Conf. on Conduction and Breakdown in Dielectric Liquids, Berlin, West Germany, pp. 398-403 (1981).

45. R. E. Hebner, "Experimental Comparison of Step-Response and Ramp-Response Measurements of Freestanding Dividers," Proc. Workshop on Measurement of Electrical Quantities in Pulse Power Systems, Nat. Bur. Stand. (U.S.), NBS Special Publication 628, 1982.

46. R. E. Hebner, E. F. Kelley, G. J. FitzPatrick, and E. O. Forster, "The Effect of Aromatic Impurities on the Positive Streamer Growth in Marcol 70," Conf. Record of 1984 IEEE Int. Symp. on Elec. Insul., June 11-13, 1984, pp. 284-287, June 1984.

Robert E. Hebner (continued)

47. R. E. Hebner and E. F. Kelley, "Electro-Optic Electric-Field Measurements Near Oil-Pressboard Interfaces, Conf. Record of 1984 IEEE Int. Symp. on Elec. Insul., June 11-13, 1984, pp. 311-314, June 1984.

48. G. J. FitzPatrick, E. O. Forster, R. E. Hebner, and E. F. Kelley, "Streamer Initiation in Liquid Hydrocarbons under Divergent Field Conditions," Annual Report 1984 Conference on Elec. Insul. and Dielectric Phen., Oct 21-25, 1984, Wilmington, Del., pp. 291-296, 1984.

49. G. J. FitzPatrick, E. O. Forster, E. F. Kelley, and R. E. Hebner, "Streamer Initiation in Liquid Hydrocarbons," 1985 Annual Report-Conference on Electrical Insulation and Dielectric Phenomena, Amherst, NY, Oct. 20-24, 1985 (Published by Inst. of Electrical and Electronic Engineers, New York) pp. 27-32, 1985.

Other

50. R. E. Hebner, "Kerr Effect, Electro-optical," in Encyclopedia of Physics, R. G. Lerner and G. L. Trigg, Ed. (Addison-Wesley Publishing Company, Inc., Reading, MA, 1981) pp. 483-484.

51. R. H. McKnight and R. E. Hebner, Editors, Proceedings of the Workshop on Electrical Measurements in Pulsed Power Systems, Nat. Bur. Stand. (U.S.), NBS Special Publication 628, 1982.

52. R. E. Hebner, "The Measurements of High Current and Voltage Pulses," Pulsed Power Lecture Series, Lecture No. 35, 45 pages, Texas Tech University, Lubbock, Texas (July 1984).

53. R. E. Hebner, Electro-optical Measurement Techniques, in "Fast Electrical and Optical Measurements," (M. Nijhoff, Boston) pp. 5-25, 1986..

GERARD N. STENBAKKEN

Education:

University of Minnesota	B.Phy. (1964)
University of Maryland	M.S. (1969)

Employment Information:

1969-present	Physicist, National Bureau of Standards
1963-1969	Engineer, Vitro Laboratories

Professional Activities:

Member, IEEE Subcommittee on Digital Techniques in Electrical Measurements, 1983-present;

Secretary/Treasurer, IEEE Washington/No.Va, Instrumentation and Measurement Chapter 1984-present.

Professional Society Memberships:

Institute of Electrical and Electronic Engineers

Publications:

1. T. M. Souders and G. N. Stenbakken, "Modeling and Test Point Selection for Data Converter Testing," 1985 IEEE International Test Conference Proceedings, IEEE Computer Society, IEEE Philadelphia Section, Nov. 19-21, 1985, Philadelphia, PA, IEEE Press, pp. 813-817 (Nov. 1985).

2. O. B. Laug, G. N. Stenbakken, and T. F. Leedy, "Electrical Performance Tests for Audio Distortion Analyzers," NBSIR 85-3269, 157 pages (Nov. 1985).

3. G. N. Stenbakken, T. M. Souders, J. A. Lechner, and P. T. Boggs, "Efficient Calibration Strategies for Linear, Time Invariant Systems," Proceedings of 1985 IEEE AUTOTESTON Conference, Uniondale, L.I., NY, 10/22-24/85, IEEE Press, NY, pp. 361-366 (Oct. 1985).

4. G. N. Stenbakken, "Dual-Channel Sampling Systems," paper for Digital Methods in Waveform Metrology Seminar, Spec. Publ. 707, pp. 55-73 (Oct. 1985).

5. G. N. Stenbakken, "A Wideband Sampling Wattmeter," IEEE Trans. Power Appar. Syst., PAS-103, No. 10, pps. 2919-2926 (Oct. 1984).

6. R. S. Turgel, N. M. Oldham, G. N. Stenbakken, and T. H. Kibalo, "NBS Phase Angle Calibration Standard," Nat. Bur. Stand. (U.S.), Tech. Note 1144, 143 pages (July 1981).

7. A. H. Sher and G. N. Stenbakken, "Selection and Application Guide to Commercial Intrusion Alarm Systems," Nat. Bur. Stand. (U.S.), Spec. Publ. 480-14, 40 pages (Aug. 1979).

8. G. N. Stenbakken, W. E. Phillips, and S. E. Bergsman, "Terms and Definitions for Intrusion Alarm Systems," Department of Justice, Law Enforcement Standards Program, LESP-RPT-0305.00, 16 pages (Oct. 1974).

DAVID L. HILLHOUSE

Education:

University of Missouri	B.S.E.E. (1950)
University of Missouri	M.S.E.E. (1952)

Employment Information:

1967-present	Physicist, National Bureau of Standards
1952-1967	Electrical Engineer, General Electric

Professional Activities:

Member, IEEE Instrument Transformers Subcommittee

Chairman, Workshop on Metering Accuracy Coupling Capacitor Voltage Transformers, 1983

Professional Society Memberships:

Institute of Electrical and Electronics Engineers
Instrument Society of America

Publications:

Journal Articles

1. D. L. Hillhouse and H. W. Kline, "A Ratio Bridge for Standardization of Inductors and Capacitors," IRE Trans. Instru., vol I-9, 1960.

2. D. L. Hillhouse, "Resonant Capacitance-Inductance Transfer," IEEE Trans. on Comm. and Elec., No. 66, 1963.

3. D. L. Hillhouse, "Circuit for Impulse Testing of Gas-Tube Lightning Arresters," IEEE Trans. Commun., vol. COM-20, pp. 936-941, 1972

4. D. L. Hillhouse and A. E. Peterson, "A 300-kV Compressed Gas Standard Capacitor with Negligible Voltage Dependence," IEEE Trans. Instru. Meas., vol.IM-22, 1973.

5. R. L. Kahler, D. L. Hillhouse, and W. E. Anderson, "A Simple Overcurrent Protection Circuit for a High Voltage Laboratory," IEEE Trans. Instru. Meas., vol. 25, pp. 161-162, 1976.

6. D. L. Hillhouse, O. Petersons, and W. C. Sze, "A Prototype System for On-Site Calibration of Coupling Capacitor Voltage Transformers (CCVTs)," IEEE Trans Power Appar. Sys., vol. PAS-98, pp. 1026-1036, 1979.

7. D. L. Hillhouse, O. Petersons, and W. C. Sze, "A Simplified System for Calibration of Coupling Capacitor Voltage Transformers (CCVTs)," IEEE Trans. Power Appar. Sys., vol. PAS-103, pp. 1092-1098, 1984.

DAVID L. HILLHOUSE (continued)

Interagency Reports

8. D. L. Hillhouse, O. Petersons, and W. C. Sze, "A Prototype Field Calibration System for Coupling Capacitor Voltage Transformers," EPRI Report No. EL-690, 1978.

9. R. E. Hebner, D. L. Hillhouse, and R. A. Bullock, "Evaluation of a Multimegavolt Impulse Measurement System," NBSIR 79-1933, 1979.

10. D. L. Hillhouse, "Guide for Safe Operating Procedures at High Voltage Substations by NBS and Utility Staff during the Field Calibration of Coupling Capacitor Voltage Transformers (CCVTs)," NBSIR 81-2192, 1981.

11. D. L. Hillhouse and D. A. Leep, "Analysis of the Calibration of Metering CCVTs in a Utility Substation," NBSIR 81-2360, 1981.

12. D. L. Hillhouse, "Effects of High-Voltage Switching on the EPRI-NBS Coupling Capacitor Voltage Transformer (CCVT) Calibration System Standard Divider," NBSIR 83-2666, 1983.

13. D. L. Hillhouse, O.Petersons, and W. C. Sze, "A Simplified System for Calibration of CCVTs in the Substation," NBS Tech Note 1155, 1984.

14. D. L. Hillhouse, "Outline of CCVT Calibration Procedure, EPRI-NBS Prototype Systems," NBSIR 84-2987, 1984.

Published Conference Papers

15. D. L. Hillhouse and W. C. Sze, "Calibration of CCVTs in the Substation," 45th Annual International Conference of Double Clients, Section 9-501, 1978.

16. D. L. Hillhouse, "The EPRI-NBS CCVT Calibration Systems," Proc. Workshop on Metering Accuracy CCVTs, June 2-3, 1983 (Published by the Electric Power Research Institute, Palo Alto, CA), pp. 7-1 to 7-25, 1985.

17. D. L. Hillhouse, "NBS Experience, Field Calibration of CCVTs, Proc. Workshop on Metering Accuracy CCVTs, June 2-3, 1983 (Published by the Electric Power Research Institute, Palo Alto, CA), pp. 1-1 to 1-14, 1985.

Other

18. D. L. Hillhouse, Portable System Calibrates CCVTs," Electric World, vol. 189, pp. 44-46, 1978.

NBS-114A (REV. 2-80)

U.S. DEPT. OF COMM. BIBLIOGRAPHIC DATA SHEET (See instructions)	1. PUBLICATION OR REPORT NO. NBSIR 86-3405	2. Performing Organ. Report No.	3. Publication Date June 26, 2986

4. TITLE AND SUBTITLE

Report of Tests on Joseph Newman's Device

5. AUTHOR(S)

R. Hebner, G. Stenbakken, D. Hillhouse

6. PERFORMING ORGANIZATION (If joint or other than NBS, see instructions)

NATIONAL BUREAU OF STANDARDS
DEPARTMENT OF COMMERCE
WASHINGTON, D.C. 20234

7. Contract/Grant No.

8. Type of Report & Period Covered

9. SPONSORING ORGANIZATION NAME AND COMPLETE ADDRESS (Street, City, State, ZIP)

U.S. Patent and Trademark Office
Crystal Gateway 2
1225 Jefferson Davis Highway
Crystal City, VA 22202

10. SUPPLEMENTARY NOTES

☐ Document describes a computer program; SF-185, FIPS Software Summary, is attached.

11. ABSTRACT (A 200-word or less factual summary of most significant information. If document includes a significant bibliography or literature survey, mention it here)

This report describes tests performed between March 1986 and June 1986 on a device submitted by Joseph Newman for testing at the National Bureau of Standards. The purpose of the testing was to determine if the output power of the device was greater than the ~~input~~ power.

12. KEY WORDS (Six to twelve entries; alphabetical order; capitalize only proper names; and separate key words by semicolons)

efficiency; electrical measurements; energy; generator; Newman; power loss

13. AVAILABILITY

☐ Unlimited
☐ For Official Distribution. Do Not Release to NTIS
☐ Order From Superintendent of Documents, U.S. Government Printing Office, Washington, D.C. 20402.
☒ Order From National Technical Information Service (NTIS), Springfield, VA. 22161

14. NO. OF PRINTED PAGES

15. Price